Linear and nonlinear optical properties of the conjugated polymers PPV and MEH-PPV

S. J. Martin, D. D. C. Bradley, P. A. Lane, and H. Mellor
Department of Physics and Astronomy, University of Sheffield, Sheffield S3 7RH, United Kingdom

P. L. Burn
Dyson Perrins Laboratory, University of Oxford, Oxford, OX1 3QY, United Kingdom
(Received 30 November 1998)

We have used absorption and electroabsorption spectroscopy to investigate the electronic structure of poly(*para*-phenylene vinylene) (PPV) and poly (2-methoxy, 5-(2′-(ethyl)hexyloxy)-*p*-phenylene vinylene) (MEH-PPV). In particular we examine the often used assumption that the electronic structure of PPV and its dialkoxy substituted derivatives are essentially the same. The absorption spectrum of PPV consists of three peaks, while that of MEH-PPV has four peaks. We discuss the controversial origin of the extra peak as well as evidence for Davydov splitting effects in the absorption spectrum of PPV. The analysis of the nonlinear spectra shows further differences between the two materials. First, the binding energy of the $1B_u$ exciton for PPV is some 0.1 eV higher than for MEH-PPV. Second, the peak value of $\mathrm{Im}\{\chi^{(3)}(-\omega;0,0,\omega)\}$ for PPV is approximately 40 times higher than that of MEH-PPV. We also found that the sum-over-states modeling of the electroabsorption spectra indicates that the transition dipole moment between the mA_g and nB_u states is of opposite sign in the two polymers. [S0163-1829(99)02523-0]

I. INTRODUCTION

Poly(para-phenylene vinylene) (PPV) and its derivatives have recently received a great deal of attention both from experimental and a theoretical perspectives.[1–3] This interest is in large part motivated by the demonstration of electroluminescence with high efficiency[3] and the very large, ultrafast, optical nonlinearities that these materials possess.[4] Critical to the existence of such effects is the presence of a delocalized π-electron system associated with the conjugated molecular backbone. In order to optimize conjugated polymers for device applications, it is important to know the energies and nature of the excited states of this π-electron system as well as how they depend on chemical and physical structure.

PPV is insoluble and thus thin films are usually prepared by thermal conversion of a soluble nonconjugated intermediate, or precursor, polymer. In order to improve its processability, many soluble derivatives of PPV have been synthesized by attaching side groups to the phenylene rings at the 2 and/or 5 positions. The chemical structures of PPV and poly(2-methoxy, 5-[2′-(ethyl)hexyloxy]-*p*-phenylene vinylene) (MEH-PPV), a widely used derivative, are shown in Fig. 1. It is a common implicit assumption that the dominant effect dialkoxy substitution has on the electronic structure of the polymer is to produce a uniform redshift of the energy of the excited states. Thus many experimental reports treat PPV and its derivatives as fundamentally equivalent. We are not aware of any previous experimental studies which have specifically examined this assumption, and an important part of the work reported here is an investigation of the location of the principal low-lying excited states of the two polymers.

Ideally, PPV and MEH-PPV have C_{2h} symmetry. As a consequence the electronic states must be of even (gerade) or odd (ungerade) parity. One-photon optical transitions are strongly allowed only between states with opposite parity. This means that half of the excited states of these materials are inaccessible by linear spectroscopies. Nonlinear optical (NLO) techniques allow these states to be investigated, but most NLO techniques require high-intensity (pulsed) laser systems for which it is difficult to obtain tunability over a wide energy range. Electroabsorption (EA) spectroscopy is particularly attractive, as it is a NLO technique that can be performed using cw light sources and thus a wide spectral range is more readily accessed. In this technique the optical absorption of a material is modulated by a low frequency ac ($\sim$kHz) electric field. The resulting spectra, to a good approximation, are proportional to the imaginary part of the dc Kerr susceptibility, $\chi^{(3)}(-\omega;0,0,\omega)$, since $\omega \sim 10^{15}$ Hz. A number of conjugated polymers have been studied by EA spectroscopy, including polyacetylene,[5] polydiacetylenes (PDA),[6] and polythieneylenevinylene (PTV).[7] In general these studies have found that the EA spectra reasonably closely follow a combination of first and second energy derivatives of the linear absorption spectrum. In addition, they observed some field-induced features corresponding to tran-

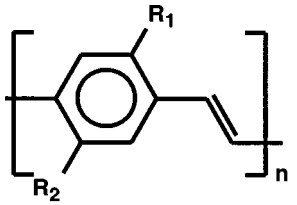

PPV: $R_1=R_2=H$

MEH-PPV: $R_1=$ 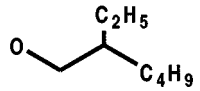

FIG. 1. Chemical structure of PPV and MEH-PPV.

sitions to states that are normally one-photon forbidden and that become partially allowed in the presence of an electric field.

The electric field leads to a mixing of states. This gives rise to two effects: First, the excited-state energies are subject to a Stark shift. For nondegenerate states and, to second order in the applied electric field, the result is a change in the optical-absorption proportional to a combination of the first and second (photon) energy derivatives of the absorption coefficient α. These have traditionally been interpreted as arising from transitions involving a change in polarizability (first derivative) and a change in permanent dipole moment (second derivative).[8–10] Second, the electric field mixes the symmetries of the excited states which results in a transfer of oscillator strength from the strongly allowed optical transitions to transitions forbidden in the absence of an electric field. The transfer of oscillator strength results in a negative spectral response proportional to the absorption coefficient (though the constant of proportionality may vary across the spectrum) together with the appearance of induced absorption bands, which are entirely unrelated to the unperturbed absorption spectrum. For real conjugated polymer samples, the situation is further complicated by the existence of a distribution of conjugation lengths. As the third-order hyperpolarizability varies with conjugation length, a distribution of conjugation lengths makes it difficult to analyze EA spectra solely in terms of derivatives of the linear absorption spectrum.

Recently, Liess *et al.*[11] modeled the EA spectra of a variety of conjugated polymers using a sum-over-states (SOS) approach incorporating three essential states and an asymmetric distribution of conjugation lengths. These three essential states are the ground state (the $1A_g$), the lowest odd-parity excited state (the $1B_u$), and an even-parity state strongly coupled to the $1B_u$ (the mA_g). While their model agrees with measured EA spectra, third-harmonic-generation measurements on PPV films[12] have detected an odd-parity three-photon state (the nB_u). This state will participate in three-photon processes, and should be included in any complete model. Indeed, Guo *et al.*[13] predicted that the third-order optical nonlinearity of conjugated polymers is dominated by contributions from all four states. We have therefore developed a SOS model incorporating four essential states and a distribution of conjugation lengths, and have used the model to describe the nonlinear optical spectra of PPV and MEH-PPV. Comparison of the results for PPV and MEH-PPV allows us to address the effect of chemical substitution on the electronic structure of this important class of conjugated polymers.

II. EXPERIMENT

The polymers were synthesized according to previously published methods.[14,15] The PPV samples used in this study were prepared via thermal conversion of films of a tetrahydrothiophenium leaving group precursor polymer. The films were converted under dynamic vacuum (10^{-5} Torr) at a temperature of 220 °C for 6 h. The MEH-PPV samples were made by spin coating from a 1% by weight solution of the polymer in toluene. Samples for UV/Vis absorption measurements were prepared by spin coating films onto spectrosil substrates. Samples for EA measurements were fabricated by spin coating films onto spectrosil substrates that had a set of interdigitated electrodes, with a finger spacing of 100 μm, predeposited on them. These electrodes were prepared by the thermal evaporation of aluminum through a shadow mask. The UV/Vis absorption spectrum of the polymers was measured at 77 K, over the spectral range 200–900 nm using a Unicam UV4 spectrophotometer equipped with a custom-built liquid-nitrogen-cooled cryostat.

The electroabsorption spectrometer consists of a light source (100-W tungsten halogen lamp, or 150-W Xe lamp), monochromated by a Digichrom DK 240 single grating monochromator equipped with a 1200-lines/mm holographic grating, a nitrogen-cooled cold finger cryostat, a high-voltage amplifier, and a silicon photodiode. The light from the monochromator was focused onto the sample, and the transmitted light was collected and focused onto the photodiode. The electrical output from the photodiode was preamplified, and split into ac and dc components. The ac component of the signal, which corresponds to the field-induced change in the transmission, ΔT, was measured using a lock-in amplifier set to the second harmonic of the field modulation. The dc component, which corresponds to the unperturbed transmission T was measured with a computer controlled voltage meter. The outputs from the lock-in and the meter are recorded by a computer and ratioed to yield the normalized change in the transmission, $\Delta T/T$. For normal incidence and neglecting multiple reflections $\Delta T/T$ is related to the electric-field-induced change in the reflectivity, ΔR, and the absorption coefficient $\Delta\alpha$ of the film, by the relation[5]

$$\frac{-\Delta T}{T} = d\Delta\alpha + \frac{2}{1-R}\Delta R, \tag{1}$$

where d is the film thickness, and R is the unperturbed reflectivity. For sufficiently thick films ($d \geqslant 100$ nm), the first term in Eq. (1) is typically more than one order of magnitude greater than the second. The second term can therefore be neglected, and we can write

$$\frac{-\Delta T}{T} \approx d\Delta\alpha. \tag{2}$$

As discussed above, the electric field causes a Stark shift of the allowed optical transitions and a transfer of oscillator strength from allowed to forbidden transitions resulting in field-induced absorptions. In the absence of the transfer of oscillator strength, the Stark shift results in an EA spectrum line shape $\Delta\alpha$ of the form[16]

$$\Delta\alpha = \frac{1}{2}\Delta p F^2 \frac{\partial\alpha}{\partial E} + \frac{1}{6}(m_f F)^2 \frac{\partial^2\alpha}{\partial E^2}, \tag{3}$$

where Δp is the change in the polarizability upon excitation, F is the applied field strength, E is the photon energy, and m_f is the permanent dipole moment of the final state (assuming that the ground state is nondipolar). Within this analysis a first-derivative-like line shape for the EA is indicative of transitions to a neutral excited state. A second derivative line shape indicates that the excited state has a significant dipole moment. Transfer of oscillator strength does occur, however, resulting in a (negative) contribution from the zeroth deriva-

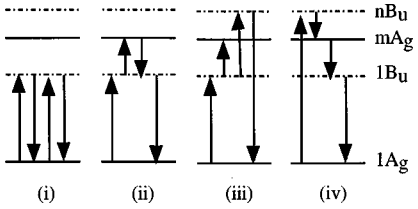

FIG. 2. Sum-over-states pathways used to calculate $\chi^{(3)}(-\omega;0,0,\omega)$.

tive (i.e., α) to the EA spectrum. This zeroth derivative contribution to the EA spectrum will also result in an apparent second derivative component, as the transfer of oscillator strength results in a small perturbation of the first derivative component which can be approximated by a second derivative in a Taylor-like expansion. Recently Liess *et al.*[11] showed that a significant contribution to the second derivative component of the EA response of conjugated polymers can also arise from the distribution of conjugation lengths that exists in most conjugated polymer systems. They showed that the EA spectra in the region of the low-lying excitations for a wide range of conjugated polymers could be interpreted solely in terms of neutral excitations.

Orr and Ward[17] showed that the third-order nonlinear susceptibilities, $\chi^{(3)}(-\omega_\sigma;\omega_1,\omega_2,\omega_3)$, can be expressed in terms of components that involve summations over sets of four states *a, b, c,* and *d.* These expressions are of the form

$$\chi^{(3)}(-\omega_\sigma;\omega_1,\omega_2,\omega_3)=\frac{N}{\varepsilon_0}\frac{e^4}{3!\hbar^3}S_T\sum_a \rho_0(a)\times\left[\sum_{\text{abcd}}\frac{\mu_{ab}\mu_{bc}\mu_{cd}\mu_{da}}{(\Omega_{ba}-\omega_\sigma)(\Omega_{ca}-\omega_2-\omega_3)(\Omega_{ba}-\omega_3)}-\sum_{\text{acd}}\frac{\mu_{ac}\mu_{ca}\mu_{ad}\mu_{da}}{(\Omega_{ca}-\omega_\sigma)(\Omega_{da}-\omega_3)(\omega_{ba}+\omega_\sigma)}\right], \tag{4}$$

where ω_1, ω_2, and ω_3 are the input radiation frequencies, and $\omega_\sigma(=\omega_1+\omega_2+\omega_3)$ is the frequency of the output radiation field. Ω_{xy} is the energy separation of the states x and y, and μ_{xy} is the transition dipole moment connecting the two states. Ideally these summations should be carried out over all combinations of all the states of the system. However, several workers have shown that for quasi-one-dimensional conjugated polymers only a few ''essential'' states need be taken into account.[13,18] These states are the ground state and the $1B_u$, the mA_g, and the nB_u excited states. mA_g is identified as that state which couples most strongly to the $1B_u$ state, and the nB_u state is associated with the onset of the continuum of states.[19] As discussed above, Liess *et al.*[11] modeled the EA spectra of several conjugated polymers using a three-essential-state model, the states used were the ground state, the $1B_u$ state, and the mA_g state. Within this model two photon pathways are included in the SOS calculation. These pathways are illustrated in parts (i) and (ii) of Fig. 2. Here we use a similar approach, but extend the model to include the nB_u state.[18] This introduces two new pathways into the SOS calculation. These pathways are shown in parts (iii) and (iv) of Fig. 2.

In order to take into account the vibronic structure in the EA spectra, the sums in Eq. (4) are carried out over the vibrational levels $\Omega_x+n\omega$ (where Ω_x is the electronic state energy, n is an integer, and ω is the vibrational quantum energy), and the dipole moments are multiplied by the relavent Franck-Condon overlap factor F_{pq}, which is given by[19,20]

$$F_{pq}(a)=\frac{e^{-a^2/4}}{\sqrt{2^{p+q}p!q!}}\sum_r \frac{2^r(-1)^{q-r}a^{p+q-2r}p!q!}{r!(p-r)!(q-r)!}, \tag{5}$$

where p and q are the phonon levels between which the transition occurs, a is the difference in configurational coordinate between the two electronic states involved, and the sum is from $r=0$ up to the smaller of p or q. To simplify the calculation we used the same vibrational quantum energy for all of the electronic states.[11,19]

The existence of a range of conjugation lengths within the polymer films results in the excited states being distributed over a range of energies. Further, since the nonlinear response is strongly dependent on the conjugation length, the longer segments within the distribution will contribute more to the overall response of the system than the shorter segments. Liess *et al.* modeled this effect by introducing an asymetric distribution function $\zeta(E')$ and calculating the function

$$\chi^{(3)}_{\text{film}}(-\omega;0,0,\omega)\propto\int_{-\delta}^{+\delta}\zeta(E')\chi^{(3)}_{\text{SOS}}(E_{1B_u}+E';E_{mA_g}+E';E_{nB_u}+E';-\omega;0,0,\omega)dE', \tag{6}$$

where $\chi^{(3)}_{\text{SOS}}$ is the SOS susceptibility including vibronic effects, and E' is the energy. For $\zeta(E')$, we use an asymmetric Gaussian function[11]

$$\zeta(E')=\frac{1.13}{B}\frac{\exp\left\{-\left[\frac{E'}{B}-\left(\frac{0.95}{1+e^u}-0.475\right)\right]^2\right\}}{1+\exp\left\{-\left[\frac{E'}{B}-\left(\frac{0.95}{1+e^u}-0.475\right)\right]\right\}}. \tag{7}$$

The parameters B and u allow the width and assymetry of ζ' to be varied without changing the position of the mean energy. The asymmetry is defined as the ratio of the energies

from the mean energy to the half-height points. Near to resonances the measured EA signal is proportional to the imaginary part of the nonlinear susceptibility $\chi^{(3)}(-\omega;0,0,\omega)$. The line shape calculated from Eq. (6) can thus be compared directly to the measured EA line shapes. We emphasize that it is the line shapes we are interested in here, as the calculation of values of $\chi^{(3)}$ requires a knowledge of the density of conjugated units within the films, the local-field tensor, and the absolute values of the various transition dipole moments, and this information is not available. The calculated line shapes allow us to interpret the spectral features in the measured spectra in terms of the essential states.

As mentioned in the Introduction EA spectroscopy can be used to investigate the nonlinear optical properties of materials. The dc Kerr susceptibility is defined by

$$\chi^{(3)}(-\omega;0,0,\omega)=\frac{\tilde{n}\Delta\tilde{n}}{2\pi F^2}, \tag{8}$$

where $\tilde{n}$ and $\Delta\tilde{n}$ are the complex refractive index and the electric-field-induced change in the complex refractive index of the film, respectively, and F is the applied electric field. The spectral dispersion of the refractive indices of the films were calculated from UV/Vis absorption spectra (neglecting interference and reflectivity effects). In this case the optical density $\mathcal{O}$ of a film can be related to the absorption coefficient, α, by

$$\alpha\approx\frac{2.302\times\mathcal{O}}{d}, \tag{9}$$

where d is the film thickness. The imaginary part of the refractive index, k, can be calculated directly, since

$$\alpha(E)=\frac{4\pi kE}{hc}. \tag{10}$$

The real part of the refractive index is then calculated via a Kramers-Kronig relation

$$n(E)-1=\frac{ch}{2\pi^2}\int_0^\infty\frac{\alpha(E')}{E'^2-E^2}dE'. \tag{11}$$

The field-induced change in the imaginary part of the refractive index, Δk, can be obtained from the EA data, since

$$\Delta k(E)=\frac{\Delta\alpha(E)hc}{4\pi E}. \tag{12}$$

If $\Delta\alpha$ is known over a wide range of photon energies, then the field-induced change in the real part of the refractive index, Δn, can be calculated using a Kramers-Kronig transform

$$\Delta n(E)=\frac{ch}{\pi}\int_0^\infty\frac{\Delta\alpha(E')}{E'^2-E^2}dE'. \tag{13}$$

$\chi^{(3)}(-\omega;0,0,\omega)$ can thus be calculated from the linear absorption and EA spectra.

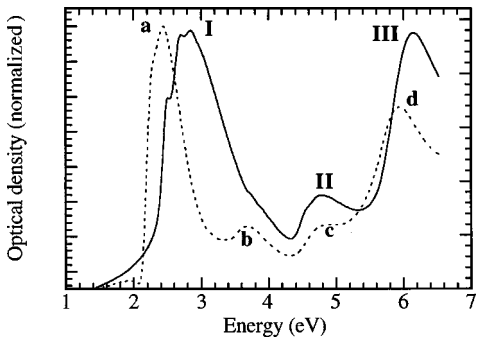

FIG. 3. Optical-absorption spectra of PPV (solid line) and MEH-PPV (dashed line).

III. RESULTS AND DISCUSSION

A. Linear absorption spectra

The linear absorption spectra measured for our samples of PPV and MEH-PPV are shown in Fig. 3. Both agree well with previous reports.[1,11,21–23] The PPV spectrum consists of two strong peaks, labeled *I* and *III*, at 2.84 and 6.15 eV, and a third, weaker, peak *II*, at 4.77 eV. At around 3.66 eV the slope of peak *I* changes, suggesting that there are at least two overlapping components contributing to peak *I*. Peak *I* has a clearly resolved vibronic progression, with a spacing of approximately 180 meV, which is typical for a carbon carbon stretching mode. Peak *II* also shows a (less well resolved) vibronic structure. The PPV absorption spectrum displays a strong tail to low photon energies. This is believed to be largely due to Rayleigh scattering of light from microcrystallites within the film. The MEH-PPV spectrum consists of two strong peaks *a* and *d*, at 2.44 and 5.94 eV and two weaker peaks *b* and *c* at 3.69 and 4.83 eV. The first peak of the MEH-PPV absorption shows poorly resolved vibronic structure in the form of two shoulders at 2.29 and 2.54 eV which are due to vibronic transitions. They are less well resolved than those in the PPV spectrum due to the disorder present in the film. It is interesting to note that the widths and shapes of these peaks are quite different in the two polymers. The full width at half maximum for peaks *I* and *a* are 1.14 and 0.56 eV. Peak *I* is significantly more asymmetric than peak *a*, even allowing for the greater degree of vibronic structure visible in peak *I*. This difference has not been emphasized previously, to our knowledge. We believe that it is related to differences in polymer chain packing. PPV is known to be a crystalline polymer, and when prepared as thin films via the precursor route forms a nanocrystalline structure.[24] The $p2_{gg}$ crystal structure would be expected to give rise to Davydov splitting of the exciton absorption. In general, when the dipole moments of two (or more) excitons are parallel, only the higher-lying Davydov component of the absorption is allowed. When they are head to tail then only the lower component is allowed. Disorder with the PPV films results in a spread in the degree of Davydov splitting, and can also result in both components being allowed. The asymmetric substitution of MEH-PPV disrupts crystallization and Davydov splitting will be greatly suppressed. Davydov splitting effects are well known in thin films of conjugated oligomers such as sexithiophene and hexaphenyl.[25,26] In these materials the degree of Davydov splitting can be

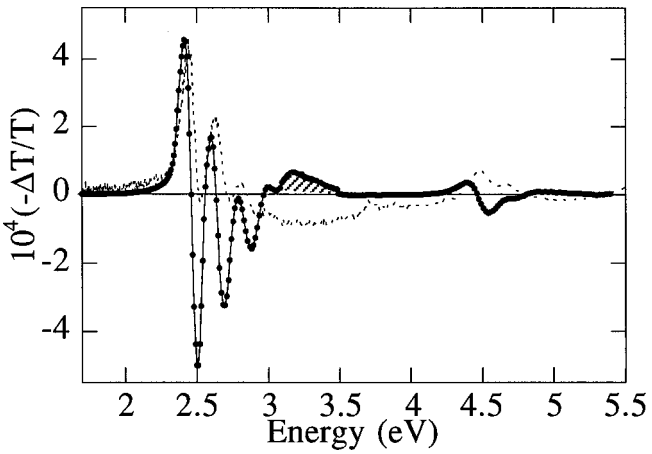

FIG. 4. EA spectrum of PPV (solid line) for an applied field strength of 50 kV/cm, and the normalized first derivative of the linear absorption spectrum (dashed line).

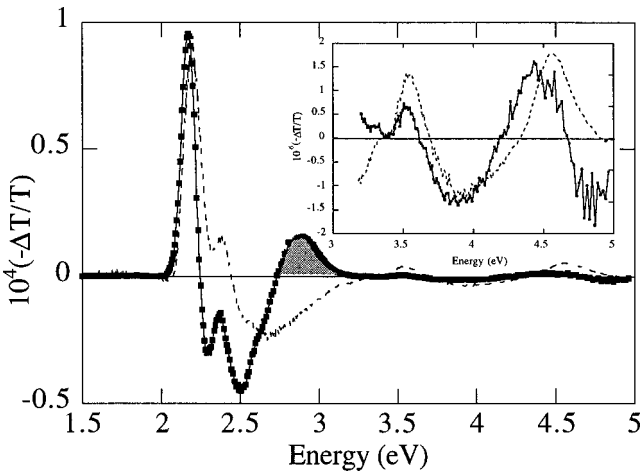

FIG. 5. EA spectrum of MEH-PPV (solid line) for an applied field strength of 50 kV/cm, and the normalized first derivative of the linear absorption spectrum (dashed line). The inset shows the spectra in the range 3.2–5.0 eV on an enlarged scale.

controlled by altering the film deposition conditions leading to strong variations in absorption spectra.

The peaks in the absorption spectra are due to different allowed excitations of the phenylenevinylene π electron system. The C_{2h} symmetry of the (ideal) polymer chains means that the ground state is of A_g symmetry, and allowed optical transitions are to states with B_u symmetry. The lowest-lying peak (*I* and *a*) is due to transitions between molecular orbitals delocalized along the polymer backbone. This transition is termed the $1A_g$ to $1B_u$ transition. Peaks *III* and *d* arise from transitions to highly localized states originating from the molecular orbitals of benzene. It is termed the $1A_g$ to $2B_{1u}$ transition. Peaks *II* and *c* are due to transitions between localized and delocalized states, and is the $1A_g$ to $2B_{2u}$ transition. The origin of peak *b* is the subject of some considerable debate. Some workers claim that this transition arises because of finite-size effects arising from structural disorder: The π-electron system of the polymer consists of segments with a distribution of conjugation lengths. Others have proposed that it arises from the effects of charge conjugation symmetry (CCS) breaking due to the dialkoxy substitution of the phenylene rings in MEH-PPV. The result of this symmetry breaking is to allow a transition that is forbidden in PPV. Comparison with the spectrum of PPV suggests that the change in the slope of peak *I* above 3.66 eV, indicating another transition could then be the result of either very weak CCS breaking arising from structural defects, or finite-size effects. It is very difficult to differentiate between these two proposals. We note, however, that site-selective fluorescence studies show that there is a distribution of conjugation lengths in both polymers, and hence absorption peaks due to finite-size effects would be expected for both polymers. We believe therefore that CCS breaking is the most likely explanation of peak *b*. We note further that dimethyl PPV, a derivative of PPV that is expected to exhibit a similar degree of CCS breaking as PPV, does not exhibit either a shoulder as seen in PPV or a peak equivalent to the peak *b* in MEH-PPV.[15] The methyl substituents disrupt the packing of the polymer chains and reduce the Davydov splitting effects considerably. It seems likely therefore that the shoulder in the absorption of PPV is related to packing effects rather than being due to finite-size effects.

B. Electroabsorption spectra

Figure 4 shows a typical EA spectrum for PPV along with the first derivative of the linear absorption. In the region of peak *I* the first peak in the EA spectrum follows the first derivative closely, but with several systematic deviations. To higher photon energies the match between the two spectra becomes poor. Between 3.1 and 3.5 eV there is a feature in the EA spectrum (the shaded region in Fig. 4) that has no corresponding feature in the derivative spectrum. It is believed that this feature is due to a previously forbidden transition that becomes allowed in the presence of the applied electric field. We will return to this point below. The EA response in the region from 3.6 to 4.2 eV is very small, indicating that any electronic states in this region have a very low polarizability. We also note that the EA response in the region of peak *II* does not match the first derivative.

A typical EA spectrum for MEH-PPV is shown in Fig. 5 along with the first derivative of the linear absorption. As expected from the linear absorption spectra the vibronic coupling effects are much less prominent in the EA spectrum of MEH-PPV than in that of PPV. This reflects the greater disorder within the MEH-PPV film. As for the PPV data, the EA response in the region of peak *a* closely matches the first derivative line shape. To higher energies the line shape deviates from the first derivative, and there is a feature in the region of 2.73 to 3.15 eV (shown shaded in Fig. 5) that is assigned to field-induced activation of a previously forbidden transition. The EA spectrum in the region of peak *b* (the inset of Fig. 5) matches the first derivative line shape quite well. It has previously been reported that the EA response of MEH-PPV in this energy region was not matched by any feature in the derivative spectra.[11,21] Liess *et al.*[11] reported that similar features are present in the EA spectra of several luminescent conjugated polymers [(dioctyloxy)-PPV (DOO-PPV) and poly(alkyl thiophene) (PAT)] but absent from that of nonluminescent polymers (PTV, PDA) and speculated that it is due to a high-energy A_g state, and that its prescence is characteristic of luminescent polymers. We see no evidence for such a feature in the EA spectrum of PPV, which is lumines-

TABLE I. Results of least-squares fitting of EA data to Eq. (14). The parameter R is the correlation coefficient for each fit.

Polymer	Fit range (eV)	a_0	a_1	a_2	R	Δp (eV/V^2/m^2)	r (Å)
PPV	2.3–2.55 (peak *I*)	−2.86*e*-4	8.83*e*-5	1.87*e*-6	0.990	2.3*e*-18	9.4
	4.2–4.9 (peak *II*)	−1.67*e*-5	−2.24*e*-7	3.55*e*-6	0.890		
	3.0–3.5 (see text)	5.80*e*-6	−2.20*e*-5	1.39*e*-6	0.492		
MEH-PPV	2.0–2.4 (peak *a*)	−7.4*e*-6	2.60*e*-6	4.227*e*-8	0.988	8.1*e*-20	1.8
	3.3–4.0 (peak *b*)	−2.694*e*-7	6.17*e*-7	1.32*e*-8	0.969		
	4.0–4.96 (peak *c*)	−4.19*e*-7	6.24*e*-7	8.45*e*-8	0.890		
	2.7–3.2 (see text)	−7.33*e*-6	−1.49*e*-6	7.82*e*-7	0.809		

cent. We believe that this feature is much better explained as being due to the Stark shift of peak *b*.

In order to investigate the origin of the various features in the EA spectra we modeled them with a linear combination of the zeroth, first, and second derivatives of the absorption $\alpha(e)$, i.e.,

$$\Delta\alpha(E)=a_0\alpha(E)+a_1\frac{\partial\alpha(E)}{\partial E}+a_2\frac{\partial^2\alpha(E)}{\partial E^2}. \qquad (14)$$

Least-squares fits of Eq. (14) to features in the EA spectra were carried out. The results of this fitting are shown in Table I. No one combination of derivatives could be found to satisfactorily fit the entire EA spectra for either polymer. Good fits could, however, be obtained over limited ranges of photon energy in the region of the various spectral features in the linear absorption. No satisfactory fit could be found for the feature between 3.1 and 3.5 eV in the PPV EA spectrum. Similarly for MEH-PPV the feature between 2.73 and 3.15 eV could not be fitted. This is further evidence that these features are associated with activation of previously forbidden transitions. Liess *et al.*[11] assigned the activated transition as the one photon forbidden $1A_g$ to mA_g state. They saw a similar feature in the EA spectra of a range of conjugated polymers (DOO-PPV, PPP, PTV) and deduced that field-induced activation of the mA_g state occurs in all conjugated polymers. It follows then that the field-induced feature in the EA spectrum of PPV should also be due to the mA_g exciton. Baker, Gelsen, and Bradley[27] measured the two photon photoluminescence excitation spectrum of PPV, and found a strong two-photon absorption feature with an onset at 2.7 eV, and a peak at 2.95 eV. Clearly these values are somewhat at variance with the location of the field-induced feature seen here. One explanation for this is that the state found in Ref. 28 is not the mA_g state but another A_g state. An alternative explanation is that since the location of the A_g state reported in Ref. 28 overlaps strongly with the vibronic progression of the $1B_u$ state then part of the EA response due to that A_g state may be masked by the response of the $1B_u$ state. Subtracting the EA response of the $1B_u$ exciton, calculated by fitting the EA response to the first derivative of the absorption, from the EA spectrum has been used by others[10,13] in order to reveal the location of an induced transition masked by the response of the $1B_u$ state. Using the fit parameters for the EA response in the region of peak *I*, we calculated the EA response of PPV and subtracted this from the measured EA response. No induced absorption in the region 2.7–3.0 eV was revealed, and much of the vibronic structure to energies higher than the upper limit of the fit range remained. We conclude from this that the A_g state reported in Ref. 27 is not the mA_g state of PPV, and that this state couples rather weakly to the $1B_u$. Interestingly the best fit for peak *II* involves a negative first derivative contribution. Fitting the response in this region with a linear combination of the zeroth and second derivatives only does not significantly change the quality of the fit. The fit to the EA response of peak *c* in MEH-PPV, which is the equivalent of peak *II*, shows a positive first derivative contribution. This implies that either peaks *II* and *c* have very different origins, which we feel is unlikely, or that the state of order within the films plays an important role in determining the fitting parameters. This will be particularly true for the PPV data since the absorption data is strongly affected by scattering.

Table I also shows that a rather good fit to the EA spectrum of MEH-PPV can be obtained in the region of peak *b*. This provides further good evidence that the feature in this region in the EA spectrum arises from a Stark shift of peak *b* rather than some high-energy A_g state.

Also shown in Table I are the changes in polarizabilities and the exciton radii implied by the derivative analysis. The values for PPV are in reasonable agreement with previously reported figures.[28,29] The values for MEH-PPV are significantly lower than those for PPV. Some of this difference may be due to the degree of order within the two films. This is because the polymer chains within the MEH-PPV film are more disordered than those in the PPV film. This results in

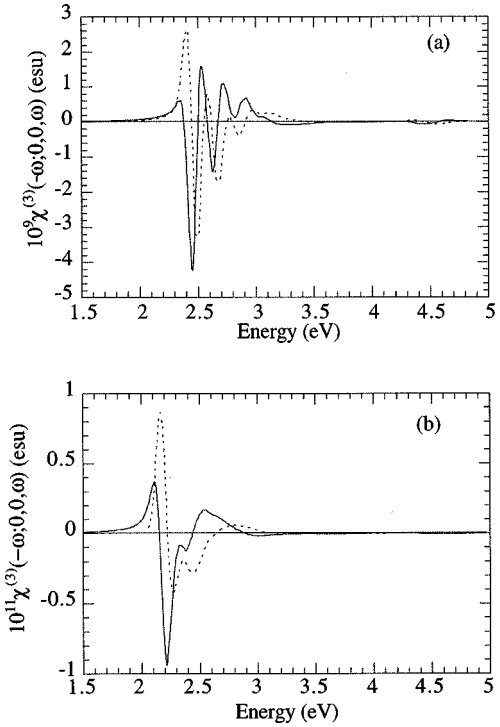

FIG. 6. Real (solid line) and imaginary (dashed line) parts of $\chi^{(3)}(-\omega;0,0,\omega)$ for (a) PPV and (b) MEH-PPV.

the MEH-PPV polymer chains being divided up into a greater range of segment sizes than in the PPV. However, EA studies of poly(phenylphenylenevinylene) (PPPV),[9] a soluble derivative of PPV which has a phenyl ring substituted onto the phenylene ring in the polymer backbone and which is much more strongly disordered than MEH-PPV, revealed values of Δp and r which were within a factor of 2 of the values for PPV. This means that disorder alone cannot account for all the differences between PPV and MEH-PPV.

C. NLO spectra

The $\chi^{(3)}$ spectra, calculated using Eqs. (3)–(8), for PPV and MEH-PPV are shown in Fig. 6. The nonlinear susceptibility for PPV is approximately 40 times larger than that for MEH-PPV. Part of this difference can be ascribed to the lower density of conjugated (i.e., $\chi^{(3)}$ active) material within the MEH-PPV polymer films. The alkoxy side groups dilute the conjugated backbone. From the linear absorption spectra we estimate that the peak absorbance for the PPV film is $\sim 4.4\times 10^5\,\mathrm{cm}^{-1}$, while for MEH-PPV it is $\sim 2.4\times 10^5\,\mathrm{cm}^{-1}$. If we assume that the absorbance per repeat unit is the same for both materials, then we can estimate that the density of conjugated units in the MEH-PPV film is about half that in the PPV film. Thus if the electronic structures of PPV and MEH-PPV are essentially the same, then we would expect the susceptibility of a MEH-PPV film to be approximately half that of a PPV film (since the NLO response is proportional to the density of conjugated units). This leaves a factor of about 20 in the magnitudes to be accounted for. The dc relative permitivities of PPV and MEH-PPV are likely to be very similar so local-field factors are not likely to play a significant role in the difference between the two polymers. As discussed above the magnitude of the EA response of

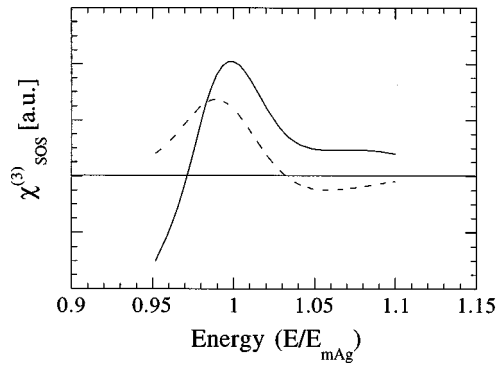

FIG. 7. Effect of vibrational features on the calculated SOS line shape in the region of the mA_g and nB_u states. The dashed line shows the line shape with no vibrational effects included in the calculation. The solid line shows the line shape with three vibrational levels included for each state.

PPPV implies that disorder cannot account for this large difference. We conclude from this that the absorbance per repeat unit is rather less for MEH-PPV than it is for PPV. This agrees with the calculations of Cornil *et al.*,[30] which looked at the effect of donor/acceptor substitution on the absorption of oligomeric models of PPV. They reported that the oscillator strength of the lowest-energy absorption of the substituted oligomers was reduced compared to the unsubstituted model compound. Unfortunately, no figures were given for the substitution induced reduction in oscillator strength.

D. SOS modeling

The SOS modeling of the EA response of these materials was limited to the region of the $1B_u$ exciton and the associated field-induced feature. This is because the other excitations of the polymers involve localized states. It is not clear at the moment whether the essential states approximation is valid for such excitations. We first address the issue of the importance of the nB_u state. Guo *et al.*[13] reported that the presence of an nB_u state would be revealed in EA spectra by a field-induced feature consisting of a $+ve$ part that is due to the mA_g, and a $-ve$ part due to the nB_u. In the absence of vibronic features SOS calculations of the type described above show such a feature (see Fig. 7). Also shown in this figure are the results of the same calculation but with the effects of vibronic coupling included. Clearly the effect of the vibrational modes is to broaden the field-induced absorption, masking the bleaching due to the nB_u. This shows that the absence of an $+ve/-ve$ field-induced feature does not preclude the presence of an nB_u state.

The results of best fits to the EA spectra of PPV and MEH-PPV are shown in Fig. 8. Table II lists the parameters used to produce these spectra. The modeled and measured EA spectra for PPV do not match as well as those for MEH-PPV. We believe this reflects the effect of the Davydov splitting discussed above on the EA spectrum of PPV films. Comparing the fit parameters for the two polymers, the first obvious difference is that the distribution of conjugations lengths used for PPV is symmetric, while that for MEH-PPV is highly asymmetric. This would appear to imply that the crystallinity of PPV results in a narrow distribution of conjugation lengths contributing to the EA spectrum. Different

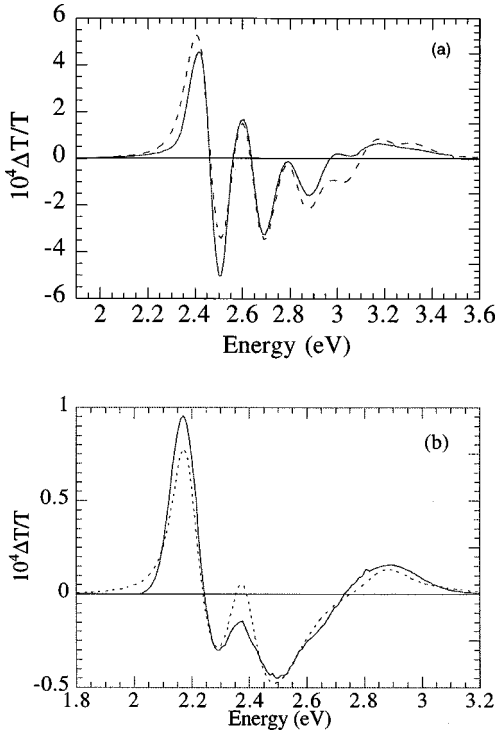

FIG. 8. Comparison of the EA (solid line) and SOS (dashed line) line shapes for (a) PPV and (b) MEH-PPV.

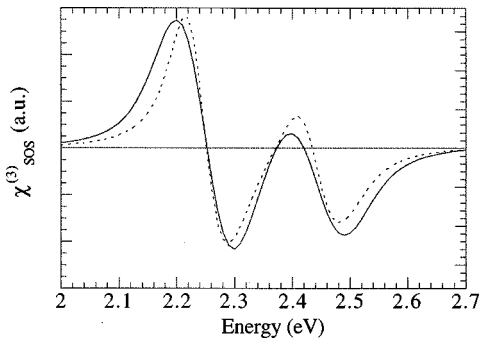

FIG. 9. Effect of the symmetry of the distribution of conjugation lengths on the position of the features in the SOS line shape. The solid line corresponds to a symmetric distribution, while the dashed line corresponds to an asymmetric distribution.

effective vibrational mode frequencies had to be used for each polymer, 185 meV for PPV and 197 meV for MEH-PPV. The value for PPV agrees well with resonant Raman studies and modeling of the linear absorption and luminescence of these polymers.[31,32] The value for the fit to MEH-PPV is surprisingly high. Resonant Raman studies of MEH-PPV show that the strong Raman modes are slightly lower in energy than the equivalent modes in PPV.[31] We would thus expect that the effective vibrational mode for MEH-PPV would be slightly lower in energy than that used for PPV. Indeed, modeling of the linear absorption spectrum of MEH-PPV in terms of sums of Gaussians by Hagler *et al.*[32] yielded an effective vibrational energy mode of 180 meV. The high phonon energy implied by the fit to the EA spectrum for MEH-PPV is related to the asymmetry of the conjugation length distribution. This is illustrated in Fig. 9, which shows the effect of varying the asymmetry of the distribution. The only difference between the two spectra in the figure is that one of them has a symmetric distribution and the other an asymmetric distribution of conjugation lengths. Note that the $+ve(-ve)$ peaks are at slightly higher(lower) energies for the symmetric distribution than the asymmetric one. For a polymer like MEH-PPV which has a broad distribution (which blurs out most of the vibronic structure) this can result in an erroneous estimate of the vibrational mode energy.

Another important difference between the two sets of parameters for the EA fits concerns the signs of the μ_{03} transition dipole moments. It was found that the μ_{03} dipole moment had to be of the same sign as μ_{23} for PPV, while for MEH-PPV these moments had to be of opposite sign. We cannot rule out the possibility that this difference arises from the Davydov splitting that affects the appearance the EA spectrum for PPV. We are not aware of any published results of calculations of these dipole moments. The energetic location of the nB_u state was found to be a much less important factor than the dipole moments involving this state. This is because of the effect of the vibronic coupling masking its position. The best fits are obtained when the nB_u state lies close in energy to the mA_g state. We conclude from this that the field-induced feature seen in the EA spectra of PPV and MEH-PPV involves contributions from the mA_g and nB_u, states but that the mA_g state dominates. The dominance of the response of the mA_g state over that of the nB_u state explains why the three essential state fits of Liess and co-workers[11,33] were so successful in reproducing the EA spectra.

Since the nB_u state is usually taken to mark the onset of the continuum of states, we can deduce a value for the binding energy of the $1B_u$ exciton in these polymers from the EA spectra. This binding energy is defined as the difference in energy between the $1B_u$ and the nB_u states. For PPV this value is 0.84 eV, and for MEH-PPV it is 0.75 eV. These values for the binding energies are considerably higher than those measured by indirect electrical methods which vary between a few meV and 0.4 eV.[2] In these indirect measurements the binding energy measured is the energy difference between the creation energy of two fully separated, geometrically relaxed, charge carriers of opposite sign and the energy of a (neutral) polaron-exciton. The binding energy measured here corresponds to the energy difference between a relaxed $1B_u$ exciton and a relaxed nB_u exciton. As pointed out by Conwell[34] care has to be taken when comparing exciton binding energies in conjugated polymers which are measured by different techniques. We note further that 0.7–

TABLE II. SOS fitting parameters used to model the EA spectra of PPV and MEH-PPV.

Polymer	E_{1b_u}	E_{mA_g}	E_{nB_u}	m_{01}	m_{12}	m_{23}	m_{03}	Q_1	Q_2	Q_3	A
PPV	2.46	3.15	3.3	1	2.2	2.5	0.07	1.	−0.7	0.7	1
MEH-PPV	2.25	2.9	3.0	1	2.2	2.0	−0.05	1.1	−0.4	0.4	2.23

0.8 eV is not significantly larger than the binding energies of approximately 0.5 eV accepted for the polydiacetylenes.[13]

It is interesting to speculate on the origin of the difference in the magnitudes of the NLO response of PPV and MEH-PPV. First, the dipole moment between the ground state and the $1B_u$ exciton may be different for the two polymers.[30] The existence of peak *b* due to CCS breaking in MEH-PPV will result in peak *a* having a smaller oscillator strength, and hence the dipole moment between the ground state and the $1B_u$ exciton will be smaller in MEH-PPV than in PPV. This dipole moment appears in all the SOS pathways, and sets the scale of magnitude for the NLO response. The smaller dipole moment in MEH-PPV also could explain the reduced Davydov splitting in the MEH-PPV films, as the magnitude of the Davydov splitting is determined by the transition dipole moment. A second factor which may affect the magnitude of the response is the dimensionality of the excitons in the polymers. The alkoxy substitution leads to an extension of the conjugation across the oxygen atoms (the mesomeric effect). This will result in the excitonic wave functions in MEH-PPV having a slightly more two-dimensional character than in PPV. Mathy *et al.*[12] showed that dimensionality can have a strong effect on the magnitude of the NLO response of organic materials.

IV. SUMMARY

In summary, we have reported the linear optical and electroabsorption properties of PPV and MEH-PPV. We find that, in keeping with other workers, the linear absorption of PPV has three well-defined transitions, while MEH-PPV has four transitions. We have presented some arguments that support the idea that the extra transition in MEH-PPV is due to CCS breaking effects and not finite length effects.

The analysis of the electroabsorption spectra indicates that PPV is significantly more nonlinear than MEH-PPV. Our SOS modeling of the EA reponse of these polymers shows that the response of the low-lying excitations can be modeled by a four-essential-state model which involves the $1A_g$, $1B_u$, mA_g, and nB_u states. The mA_g and nB_u states appear to lie very close to each other in energy. The location of the nB_u in PPV implied by the SOS fitting to the EA spectrum (3.3 eV) is in reasonable agreement with the value of 3.2 eV reported by Mathy *et al.*[12] which was measured using third-harmonic generation. The inclusion of vibrational coupling in the calculation masks the response of the nB_u state. It was not necessary to include an A_g state that lies between the $1B_u$ and mB_g states which was reported in Ref. 28. The SOS modeling also indicates that the transition dipole moment between the mA_g and nB_u states is of opposite sign in the two polymers. These results show that PPV and MEH-PPV (and other dialkoxy derivatives of PPV) are not necessarily as similar as previously assumed, and we urge caution when interpreting results from one polymer to predict the behavior of the other. We have also shown that a feature in the EA spectrum of MEH-PPV which was assigned to a previously unreported A_g state by Liess *et al.*[11] can be more convincingly assigned to the Stark shift of a high-lying nB_u state.

ACKNOWLEDGMENTS

We thank Toshiba Corporation, the Engineering and Physical Sciences Research Council of the U.K. (Grants Nos. GR/L70646 and GR/L84209), and the Commission of the European Community (TMR Network EUROLED) for their support of this work. We thank Martin Liess for useful discussions. H.M. thanks the University of Sheffield for support and D.D.C.B. thanks the Royal Society for support.

[1] J. H. Burroughes, D. D. C. Bradley, A. R. Brown, R. N. Marks, K. Mackay, R. H. Friend, P. L. Burn, and A. B. Holmes, Nature (London) **347**, 539 (1990).

[2] J.-L. Brédas, J. Cornil, and A. J. Heeger, Adv. Mater. **8**, 447 (1996).

[3] D. D. C. Bradley, Curr. Opin. Solid State Mater. Sci. **1**, 789 (1996).

[4] Y. Pang, M. Samoc, and P. N. Prasad, J. Chem. Phys. **94**, 5282 (1991).

[5] S. D. Phillips, R. Worland, G. Yu, T. Hagler, R. Freedman, Y. Cao, V. Yoon, J. Chiang, W. C. Walker, and A. J. Heeger, Phys. Rev. B **40**, 9751 (1989).

[6] L. Sebastian and G. Weiser, Phys. Rev. Lett. **46**, 1156 (1981).

[7] O. M. Gelsen, D. D. C. Bradley, H. Murata, N. Takada, T. Tsutsui, and S. Saito, J. Appl. Phys. **71**, 1064 (1992).

[8] L. Sebastian and G. Weiser, Chem. Phys. **61**, 125 (1981).

[9] Á. Horváth, H. Bässler, and G. Wieser, Phys. Status Solidi B **173**, 755 (1992).

[10] S. Jeglinski and Z. V. Vardeny, Synth. Met. **49-50**, 509 (1992).

[11] M. Liess, S. Jeglinski, Z. V. Vardeny, M. Ozaki, K. Yoshino, Y. Ding, and T. Barton, Phys. Rev. B **56**, 15 712 (1997).

[12] A. Mathy, K. Ueberhofen, R. Schenk, H. Gregorius, R. Garay, K. Müllen, and C. Bubeck, Phys. Rev. B **53**, 4367 (1996).

[13] D. Guo, S. Mazumdar, S. N. Dixit, F. Kajzar, F. Jarka, Y. Kawabe, and N. Peyghambarian, Phys. Rev. B **48**, 1433 (1993).

[14] S. H. Askari, S. D. Rughooputh, and F. Wudl, Synth. Met. **29**, 129E (1989).

[15] P. L. Burn, D. D. C. Bradley, R. H. Friend, D. A. Halliday, A. B. Holmes, R. W. Jackson, and A. Kraft, J. Chem. Soc., Perkin Trans. **1**, 3225 (1992).

[16] L. Sebastian and G. Weiser, Chem. Phys. **61**, 125 (1981).

[17] B. J. Orr and J. F. Ward, Mol. Phys. **20**, 513 (1971).

[18] D. Guo, S. Mazumdar, D. Neher, G. I. Stegeman, and W. Torruellas, in *Organic Materials for Nonlinear Optics III*, edited by G. J. Ashwell and D. Bloor (Royal Society of Chemistry, Cambridge, 1993).

[19] D. Mukhopadhyay and Z. G. Zoos, J. Chem. Phys. **104**, 1600 (1996).

[20] Z. G. Zoos and D. Mukhopadhay, J. Chem. Phys. **101**, 5515 (1994).

[21] J. M. Leng, S. Jeglinski, X. Wei, R. E. Benner and Z. V. Vardeny, Phys. Rev. Lett. **72**, 156 (1994).

[22] P. L. Burn, D. D. C. Bradley, A. R. Brown, R. H. Friend, D. A. Halliday, A. B. Holmes, A. Kraft, and J. H. F. Martens, *Elec-*

tronic Properties of Polymers: Orientation and Dimensionality of Conjugated Systems, Springer Solid State Science, Vol 107 (Springer, New York, 1992), p. 293.

[23] T. W. Hagler, K. Pakbaz, and A. J. Heeger, Phys. Rev. B **49**, 10 968 (1994).

[24] D. D. C. Bradley, Polym. Int. **26**, 3 (1991).

[25] A. Yassar, G. Horowitz, P. Valat, V. Wintgens, M. Hmyene, F. Deloffre, P. Srivastava, P. Lang, and F. Garnier, J. Phys. Chem. Adv. Mater. **99**, 9155 (1995).

[26] D. Oelkrug, H. Egelhaaf, J. Gierschner, and A. Tompert, Synth. Met. **76**, 249 (1996).

[27] C. J. Baker, O. M. Gelsen, and D. D. C. Bradley, Chem. Phys. Lett. **201**, 127 (1993).

[28] O. M. Gelsen, Ph.D. thesis, Cambridge University, 1993.

[29] O. M. Gelsen, D. A. Haliday, D. D. C. Bradley, P. L. Burn, A. B. Holmes, H. Murata, T. Tsutsui and S. Saito, Mol. Cryst. Liq. Cryst. **216**, 117 (1992).

[30] J. Cornil, D. A. d. Santos, D. Beljonne, and J. L. Brédas, J. Phys. Chem. **99**, 5604 (1995).

[31] F. H. Long, D. McBranch, T. W. Hagler, J. M. Robinson, and B. I. Swanson, Mol. Cryst. Liq. Cryst. **256**, 121 (1994).

[32] T. W. Hagler, K. Pakbaz, K. F. Voss, and A. J. Heeger, Phys. Rev. B **44**, 8652 (1991).

[33] M. Liess, S. Jeglinski, P. A. Lane, and Z. V. Vardeny, Synth. Met. **84**, 891 (1997).

[34] E. M. Conwell, Synth. Met. **83**, 101 (1996).